[7]Baldwin, B. S., and Lomax, H., "Thin Layer Approximation and Algebraic Model for Separated Turbulent Flows," AIAA Paper 78-257, 1978.

[8]Lamer, W. E., "Effects of Buffeting and Other Transonic Phenomena," AGARD-CP-187, 1976.

[9]Brandeis, J., "Flow Separation in Shear-Layer-Driven Cavities," *AIAA Journal*, Vol. 20, No. 7, 1981, pp. 908–914.

[10]Kim, I., and Chokani, N., "Navier–Stokes Study of Supersonic Cavity Flowfield with Passive Control," *Journal of Aircraft*, Vol. 29, Feb. 1992, pp. 217–223.

[11]Chen, C. L., Chow, Y. C., Van Dalsem, W. R., and Holst, T. L., "Computation of Viscous Transonic Flow Over Porous Airfoils," *Journal of Aircraft*, Vol. 26, Dec. 1989, pp. 1067–1075.

[12]Chokani, N., and Squire, L. C., "Passive Control of Shock/Boundary Layer Interactions: Numerical and Experimental Studies," *Symposium Transsonicum III*, Gottingen, Germany 1989, pp. 24–27.

[13]Tijdeman, H., "Investigation of the Transonic Flow Around Oscillating Airfoils," National Aerospace Lab., NLR TR-77-090U, The Netherlands, 1977.

[14]McDevitt, J. B., Levy, L. L., Jr., and Deiwert, G. S., "Transonic Flow About a Thick Circular-Arc Airfoil," *AIAA Journal*, Vol. 14, No. 5, 1976, pp. 606–613.

[15]Levy, L. L., Jr., "Experimental and Computational Steady and Unsteady Transonic Flows About a Thick Airfoil," *AIAA Journal*, Vol. 16, No. 6, 1978, pp. 564–572.

[16]Edwards, J. W., and Thomas, J. L., "Computational Methods for Unsteady Transonic Flows," *Unsteady Transonic Aerodynamics*, edited by D. Nixon, Vol. 120, Progress in Astronautics and Aeronautics, AIAA, Washington, DC, 1989, pp. 211–261.

Rise of Total Pressure in Frictional Flow

R. I. Issa*
Imperial College,
London SW7 2BX, England, United Kingdom

Introduction

ONE of the first basic principles introduced to students of fluid mechanics is Bernoulli's equation and its consequence on the conservation of total pressure in inviscid flow. Flows with friction, on the other hand, are known to result in a net loss of total pressure. Such loss, however, is always considered in the context of global changes occurring over macroscopic control volumes that are of interest in normal engineering applications. Thus, many if not most practitioners of fluid mechanics have come to assume that total pressure is an upper-bounded quantity, being conserved in inviscid flow, and can only decrease in frictional flow.

With the advent of modern computational methods for solving the Navier–Stokes equations, full flowfield calculations are now commonplace. In many of these computations, which often incorporate models accounting for turbulence, values of the total pressure, especially around stagnation points in external aerodynamics and on blades in cascades, have been observed to be higher than the corresponding incident freestream values. This occurs even in highly turbulent flows, when frictional effects are expected to substantially reduce total pressure. Such increase has hitherto been assumed to be due to numerical errors contaminating the solution.

In this Note, it is shown that the expectation that total pressure in frictional flow is everywhere bounded by a maximum value that equals that of the incident freestream is in fact erroneous. It is reasoned and demonstrated that the total pressure can indeed increase locally, especially around stagnation points, beyond the freestream value. It is also shown that, surprisingly, this increase is directly proportional to the viscosity.

The analysis offered here first derives a transport equation for total pressure from the Navier–Stokes equations; such an equation appears in standard text books like Ref. 1 where it is pointed out that gradients in stresses in the equation result in gradients in total pressure. It is argued here that these stress gradients can indeed act as a positive source. Two known exact solutions to the Navier–Stokes equations, namely, those of plane stagnation flow and Stokes flow around a sphere, are then considered. The exact solutions for the total pressure fields for these cases are then formulated and presented.

Governing Equations

We first examine in general the variations of total pressure as governed by the transport equations. Consider the momentum equations in multidimensions for an incompressible fluid. In Cartesian tensor notation these can be written as

$$\frac{\partial}{\partial x_j}(\rho u_j u_i) = -\frac{\partial p}{\partial x_i} + \frac{\partial \sigma_{ij}}{\partial x_j} \tag{1}$$

where σ_{ij} is the stress tensor. Multiplication of Eq. (1) by u_i gives

$$u_i\frac{\partial}{\partial x_j}(\rho u_j u_i) = -u_i\frac{\partial p}{\partial x_i} + u_i\frac{\partial \sigma_{ij}}{\partial x_j} \tag{2}$$

which can be reformulated as

$$\frac{\partial}{\partial x_j}\left(\rho u_j \frac{u_i u_i}{2}\right) = -\frac{\partial}{\partial x_i}(u_i p) + u_i\frac{\partial \sigma_{ij}}{\partial x_j} \tag{3}$$

In arriving at Eq. (3), the continuity condition for incompressible fluids

$$\frac{\partial u_i}{\partial x_i} = 0$$

has been invoked. Equation (3) can be rearranged to give

$$\frac{\partial}{\partial x_j}\left[u_j\left(p + \rho\frac{u_i u_i}{2}\right)\right] = u_i\frac{\partial \sigma_{ij}}{\partial x_j}$$

or

$$\frac{\partial}{\partial x_j}(u_j p_t) = u_i\frac{\partial \sigma_{ij}}{\partial x_j} \tag{4}$$

where the total pressure p_t is defined as

$$p_t = p + \rho\frac{u_i u_i}{2}$$

Equation (4) is a transport equation governing the total pressure. In inviscid flow, the right-hand side of the equation vanishes, thus dictating that the total pressure is constant along each streamline.

In viscous flow, however, the right-hand side of Eq. (4) can, in principle, lead to an increase in total pressure, depending on the sign of the term, which can be written as

$$u_i\frac{\partial \sigma_{ij}}{\partial x_j} = \underbrace{\frac{\partial}{\partial x_j}(u_i\sigma_{ij})}_{\text{I}} - \underbrace{\sigma_{ij}\frac{\partial u_i}{\partial x_j}}_{\text{II}} \tag{5}$$

Term II in Eq. (5) stands for dissipation and will always act as a negative source. Term I, however, is a redistribution term and can be either positive or negative.

If one integrates Eq. (4) over the flow domain, the integral of term I vanishes when no work is imparted to the fluid at the boundaries. Term II will always have a negative sign, hence leading to a net loss of total pressure over the domain. There is no reason, however, why locally term I should not be positive and greater in magnitude than term II, thereby giving a local rise in total pressure. This rise can only happen at the expense of depletion of total pressure eleswhere in the flow as mechanical energy is redistributed due to the stresses.

In what follows, the previous conjecture is verified by consideration of two flows for which analytic solutions exist.

Received Feb. 22, 1994; revision received May 3, 1994; accepted for publication May 3, 1994.

*[Job Title] Department of Mechanical Engineering.

Plane Stagnation Flow

The flow configuration is shown in Fig. 1. The exact solution was first obtained by Heimenz and is documented by Schlichting.[2] This solution is obtained by assuming that

$$u = xf'(y) \tag{6}$$

$$v = -f(y) \tag{7}$$

$$p_0 - p = \tfrac{1}{2}\rho a^2[x^2 + F(y)] \tag{8}$$

where a is a constant, and both f and F are functions of y only. The quantity p_0 stands for the value of pressure at the stagnation point. Substitution of Eqs. (6–8) into the momentum equations yields two ordinary differential equations, the solution of which gives f and F; this solution is tabulated numerically in Ref. 2.

Let us first examine the behavior of the source term $u_i(\partial\sigma_{ij}/\partial x_i)$ in the total pressure equation, Eq. (4), along the stagnation streamline ($x = 0$). It can be shown that, with the assumptions in Eqs. (6–8), the term becomes

$$u_i\frac{\partial\sigma_{ij}}{\partial x_j} = \mu f f'' \tag{9}$$

From the tabulated values of f and f'' in Ref. 2, both of these quantities are always positive. Hence, along the stagnation streamline, there is a positive source dictating the continuous increase of total pressure as the fluid approaches the stagnation point. It is interesting to note that this source arises solely from the action of the normal stresses. Also, the magnitude of the term is directly proportional to the viscosity. Next, we examine the field of total pressure p_t over the domain. Now

$$p_t = p + \tfrac{1}{2}\rho(u^2 + v^2)$$

and from Eqs. (6) and (8), and the ordinary differential equation linking f to F, we can derive the following relationship:

$$p_t = p_0 + \tfrac{1}{2}\rho[x^2(f'^2 - a^2) - 2\nu f'] \tag{10}$$

Far upstream, i.e., at $y = \infty$, $f' = a$ and $p_t = p_{t\infty}$. Hence,

$$p_{t\infty} = p_0 - \rho\nu a \tag{11}$$

Hence, from Eqs. (10) and (11), we have

$$p_t - p_{t\infty} = \tfrac{1}{2}\rho[x^2(f'^2 - a^2) - 2\nu(f' - a)] \tag{12}$$

Furthermore, far upstream, i.e., at $y \doteq y_\infty = \delta$, the freestream velocity V_∞ is given by

$$V_\infty = a\delta \tag{13}$$

With this relation, Eq. (12) can be written in the nondimensional form

$$\frac{p_t - p_{t\infty}}{\frac{1}{2}\rho V_\infty^2} = \left(\frac{x}{\delta^2}\right)^2\left(\frac{f'^2}{a^2} - 1\right) - \frac{2}{Re}\left(\frac{f'}{a} - 1\right) \tag{14}$$

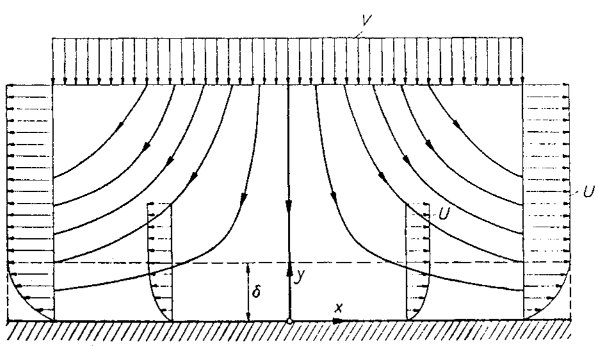

Fig. 1 Plane stagnation flow.

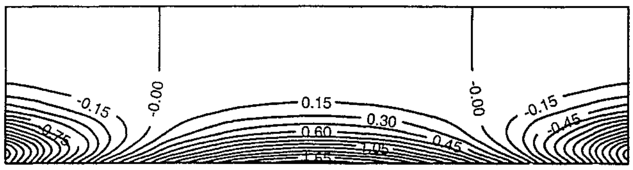

Fig. 2 Total pressure field in plane stagnation flow, *Re* = 1.

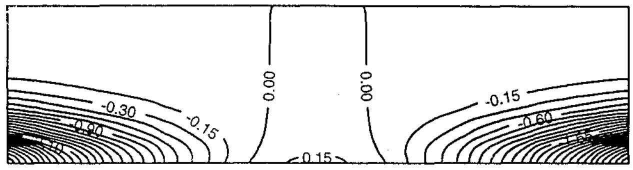

Fig. 3 Total pressure field in plane stagnation flow, *Re* = 1 × 10[1].

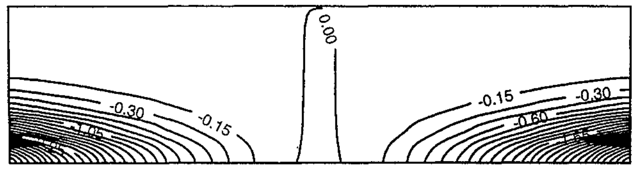

Fig. 4 Total pressure field in plane stagnation flow, *Re* = 1 × 10[2].

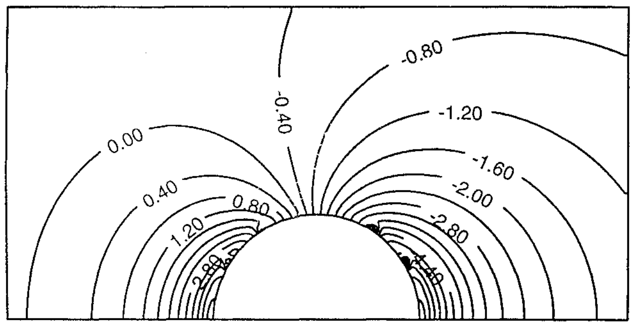

Fig. 5 Total pressure field in creeping flow around a sphere, *Re* = 1.

where

$$Re \equiv \frac{V_\infty\delta}{\gamma}$$

Contours of $(p_t - p_{t\infty})/\frac{1}{2}\rho V_\infty^2$ given by Eq. (14) are plotted in Figs. 2–4 for $Re = 1$, 1×10^1, and 1×10^2 over a domain extending over $-2 \le (x/\delta) \le 2$ and $0 \le (y/\delta) \le 1$ using the values of f'/a tabulated in Ref. 2. It is clear from the figures that around the stagnation streamline the rise in total pressure is fairly significant, with the higher values occurring at the lower Reynolds numbers; the maximum value of total pressure is attained at the stagnation point. Obviously the rise is achieved at the expense of depletion elsewhere, and overall the net change in total pressure is a negative one.

Stokes Flow

Another flow for which an exact solution is known is the creeping flow around a sphere, the so-called Stokes flow. Here we only examine the plane that passes through the center of the sphere and is aligned with the flow. The exact solution on this plane (see Ref. 2) is

$$u = U_\infty\left[\frac{3}{4}\frac{Rx^2}{r^3}\left(\frac{R^2}{r^2} - 1\right) - \frac{1}{4}\frac{R}{r}\left(3 + \frac{R^2}{r^2}\right) + 1\right] \tag{15}$$

$$v = U_\infty\frac{3}{4}\frac{Rxy}{r^3}\left(\frac{R^2}{r^2} - 1\right) \tag{16}$$

$$w = 0 \tag{17}$$

$$p - p_\infty = -\frac{3}{2}\mu\frac{U_\infty Rx}{r^3} \tag{18}$$

where $r = \sqrt{x^2 + y^2}$, R is the radius of the sphere, and x and y are Cartesian coordinates with origin at the center of the sphere.

From these equations, the expression for total pressure can be derived. It is

$$\frac{p_t - p_{t\infty}}{\frac{1}{2}\rho U_\infty^2} = \left[\frac{3}{4}\frac{Rx^2}{r^3}\left(\frac{R^2}{r^2} - 1\right) - \frac{1}{4}\frac{R}{r}\left(3 + \frac{R^2}{r^2}\right) + 1\right]^2 + \left[\frac{3}{4}\frac{Rxy}{r^3}\left(\frac{R^2}{r^2} - 1\right)\right]^2 - 1 - \frac{6}{Re}\frac{R^2 x}{r^3} \tag{19}$$

where $Re \equiv (2\rho U_\infty R)/\mu$ and $p_{t\infty}$ is the value of total pressure far upstream.

Contours of $(p_t - p_{t\infty})/\frac{1}{2}\rho U_\infty^2$ given by Eq. (19) are plotted in Fig. 5 for $Re = 1$, above which the exact solution becomes invalid. Once again it is clear that the total pressure can undergo a local increase that in this case is substantial. Here also the rise in total pressure is proportional to the viscosity as can be deduced from Eq. (19).

Conclusions

The common assumption that the total pressure can only decrease everywhere in frictional flow is an erroneous one. It is shown by examining the total pressure transport equation that stresses can, in principle, result in a local rise in total pressure; the mechanism by which this happens is the redistribution of mechanical energy by the action of these stresses. This is demonstrated for two classical flow cases for which exact solutions exist. It is found that the rise in total pressure is directly proportional to the viscosity. This implies that total pressure could indeed increase in turbulent flows more than in laminar ones becuse of the higher effective viscosity/stresses.

References

[1]Cebeci, T., and Bradshaw, P., *Momentum Transfer in Boundary Layers*, Hemisphere, New York, 1977.

[2]Schlichting, H. *Boundary Layer Theory*, McGraw-Hill, New York, 1966.

Relationship Between Transition and Modes of Instability in High-Speed Boundary Layers

Jamal A. Masad
High Technology Corporation,
Hampton, Virginia 23666

Introduction

A RELATIONSHIP exists between the different laminar-flow instability mechanisms in both low- and high-speed boundary-layer flows on aerodynamic surfaces and the breakdown of the laminar flow to turbulence. However, the details of this relationship are not well understood, particularly for high-speed flows. The most common approach for relating instability to transition is the use of the empirical N factor method, in which transition is assumed to occur whenever the integral of the linear growth rate of any instability wave reaches a certain value that is close to 9 in two-dimensional flows. In high-speed flows, the instability is complicated by the possible existence of higher modes of instability in addition to the single mode of instability [the Tollmien–Schlichting (T-S) wave] that exists in low-speed flows.

Received Oct. 29, 1993; revision received May 10, 1994; accepted for publication May 10, 1994.

*Research Scientist. Senior Member AIAA.

Mack[1] determined through numerical studies that whenever the mean flow relative to the disturbance phase velocity is supersonic over some portion of the boundary-layer profile, an infinite number of wave numbers corresponds to a single phase velocity. He called the additional disturbances "the higher modes." Mack called the first of the higher modes the second mode, which is also referred to in the literature as the Mack mode. The originally known mode that corresponds to that in incompressible flow is called the first mode. In this work, we examine the relationship between transition and modes of linear instability in both adiabatic and cooled high-speed flows over a flat plate.

Notation

In all calculations and results presented in this work, the quasi-parallel spatial stability theory is used, and therefore the frequency of the disturbance is real, whereas the spatial eigenvalue is complex. The growth rate of the wave is denoted by $-\alpha_i$, and it is made nondimensional with respect to the length scale $\delta_r^* = \sqrt{\nu_\infty^* x^* / U_\infty^*}$ such that $\alpha = \alpha^* \delta_r^*$. The dimensional freestream kinematic viscosity is denoted by ν_∞^*. The spanwise wave number parameter B is defined as $B = 1000\beta/R$ and is fixed for the same physical wave as it propagates downstream. The nondimensional spanwise wave number is $\beta = \beta^* \delta_r^*$, and β^* is the dimensional spanwise wave number of the wave. The stability Reynolds number is $R = U_\infty^* \delta_r^* / \nu_\infty^* = \sqrt{Re_x}$. The frequency parameter F is defined as $F = 2\pi f^* \nu_\infty^* / U_\infty^{*2}$, where f^* is the dimensional frequency in cycles per second (Hz) and is related to the dimensional circular frequency ω^* through $\omega^* = 2\pi f^*$. Therefore, $\omega = \omega^* \delta_r^* / U_\infty^*$ is related to F through $\omega = FR$. The specific heat at constant pressure is assumed constant, and the Prandtl number is fixed at 0.72. The dynamic viscosity varies with temperature in accordance to the Sutherland formula.

From both a practical and an experimental point of view, the wall temperature is more easily fixed than the heat flux. Therefore, we express the level of heat transfer by specifying the ratio T_w/T_{ad}, where T_w is the actual wall temperature made nondimensional with respect to T_∞^*, and T_{ad} is the adiabatic wall temperature also made nondimensional with respect to T_∞^*. If $T_w/T_{ad} = 1$, then the wall is adiabatic; if $T_w/T_{ad} < 1$, then the wall is cooled; if $T_w/T_{ad} > 1$, then the wall is heated. For first-mode waves in supersonic adiabatic boundary layers, Mack[1] found that oblique three-dimensional waves are more unstable than two-dimensional waves. Cooling has a stabilizing influence on the two- and three-dimensional first-mode waves.

Results

The most amplified second-mode waves are two-dimensional. Although cooling stabilizes first-mode waves, it has the opposite effect on the most amplified (over all frequencies) second-mode waves and destabilizes them. Heating, rather than cooling, stabilizes second-mode waves. Because second-mode waves are significant at high Mach numbers where the adiabatic wall temperatures are already large in terms of existing materials, heating is not practical in stabilizing the flow at high Mach numbers. Shaw and Duck[2] showed that at a freestream Mach number of 4 and when the cooling level exceeds a certain value, the inviscid maximum growth rate of second-mode waves starts decreasing. Our viscous calculations at the same Mach number, $R = 1.5 \times 10^3$, and $T_\infty = 120$ K show a similar effect (Fig. 1). However, our viscous calculations at $R = 1.5 \times 10^3$ and at the hypersonic Mach number of 10 showed that this reversal in the effect of cooling does not take place even with cooling levels as low as $T_w/T_{ad} = 0.02$ at $T_\infty = 50$ K and $T_w/T_{ad} = 0.01$ at $T_\infty = 300$ K.

When the first mode is responsible for transition, cooling the surface delays transition. However, cooling the surface destabilizes the second mode. Beyond a certain level of cooling, the second mode causes transition, and further cooling causes the location of transition to move upstream (Fig. 2). The results shown in Fig. 2 indicate clearly that by applying cooling to the flat plate, the instability mode responsible for transition switches from a first to a second mode. As the flat plate is cooled, the predicted transition location moves downstream and, with sufficient cooling, starts to move upstream. In Fig. 2 at a Mach number of 5, the switch from the first to the